SINGLE PASS COLLIDER MEMO CN-303

AUTHOR: P. Bambade DATE: June 10, 1985

TITLE: BEAM-BEAM DEFLECTIONS TO MEASURE SIZE SPOT AND OFFSET AT SLC IP

SLAC-CN--303

DE85 014285

PART 1 : CALCULATIONS

As soon as two SLC beams make it to the IR, both transverse offsets, spot sizes and shapes can be extracted from the pattern of angular deflections produced by the electromagnetic interaction of the two beams, as one is scanned across the other. These deflections, measured in two high resolution Beam Position Monitors (BPM) mounted symmetrically on both sides of the IP (Fig.1), will produce detectable signals allowing spot sizes to be tuned, even with the very low luminosities expected at turn on. They will also furnish a good signal to monitor beam centering and will therefore become an important part of the FFS feedback system.

This note summarizes the formulae which will allow us to correlate BPM offset readings with the properties of the two beams, and describes the range and limitations of the technique in the case of SLC.

Further work needed includes simulations, specifications for the feedback system, such as its algorithm, veto conditions and so on, aswell as integration of the beamstrahlung signal into the diagnostic scheme.

I Basic Principle

The angular deflection produced by the interaction of a SLC beam with the electromagnetic field of its colliding partner (see fig. 1) is easily expressed in the simplified case of a round target beam and a point size probe

$$\theta(\Delta) = \frac{-2r_e N_T}{\gamma} \quad \frac{1-\exp\left[\frac{-\Delta^2}{2\sigma_T^2}\right]}{\Delta} \tag{1}$$

where r_e is the classical radius of the electron, γ the relativistic factor, N_T the number of particles in the target, σ_T its RMS transverse size, and Δ the impact parameter of the probing charge.

Deflection versus impact parameter is shown in fig. 2 for targets with 2.5 and 10 μm

transverse spot sizes respectively.

The basic principle of the method is three-fold:

1. Initial beam finding: One beam — the probe in this case — is temporarily suppressed and BPM readings are compared before and after. In the case of initially large impact parameters, the magnitude of the difference is inversely proportional to the transverse offset at collision point and its sign tells in which direction to steer.
2. Beam centering: Scanning the probe across the target and recording a plot similar to fig. 2 will allow optimal centering of the two, by looking for the zero deflection symmetry point.
3. Spot size tuning: Since the slope of the deflection at the above mentionned symmetry point is inversely proportional to the transverse cross-section of the target, the same measured plot will allow spot sizes to be infered and thus minimized.

In all three cases, the sensitivity of the method is based on the fact that relative rather than absolute position information is used.

Of course, the simplifying assumption of round target and point size probe is not likely to be satisfied, and the problem therefore needs to be parametrized in two dimensions.

II Formulae

The following results are valid for collisions between gaussian, un- pinched beams.

a. Deflection of point charge

The deflection of a point charge colliding with a target consisting of a two dimensional gaussian charge distribution can be written (1,2)

$$\theta_{x,y} = \frac{-2r_e a, N_T}{\gamma} \Delta_{x,y} \int_0^\infty \frac{\exp\left[-\left(\frac{\Delta_x^2}{2\sigma_{T_x}^2+t} + \frac{\Delta_y^2}{2\sigma_{T_x}^2+t}\right)\right]}{\left(2\sigma_{T_{x,y}}^2+t\right)^{3/2}\left(2\sigma_{T_{y,x}}^2+t\right)^{1/2}} dt \qquad (2)$$

The aspect ratio is defined by $f = \sigma_{T_y}/\sigma_{T_x}$. For $f = 1$, (2) reduces to (1).

The two deflection angles are shown in fig. 3 – 5 as a function of impact parameters in both planes, for $N_T = 5 \cdot 10^{10}$ particles. Figures 3.a,b and 4.a,b correspond to round beams ($f = 1$) with $\sigma_{T_{x,y}} = 2.5$ and $7.5\,\mu$m respectively, whereas fig. 5.a,b correspond to a flat target with $\sigma_{T_x} = 25.0\,\mu$m and $\sigma_{T_y} = 2.5\,\mu$m ($f = 0.1$). Note the change in vertical scale going from fig. 3 and 4 to 5.

In the limit of large impact parameters, both target and probe are well approximated by point charges and (2) reduces to

$$\theta_{x,y} \simeq \frac{-4r_e N_T}{\gamma} \quad \frac{\Delta_{x,y}}{\Delta_x^2 + \Delta_y^2} \tag{3}$$

Turning off one of the two beams and comparing BPM readings before and after then allows, via (3), to measure initial offsets.

Taking the limit for small impact parameters gives the linear dependance

$$\theta_{x,y} \simeq \frac{-2r_e N_T}{\gamma} \quad \frac{\Delta_{x,y}}{\sigma_{T_{x,y}}(\sigma_{T_x} + \sigma_{T_y})} \tag{4}$$

Measurement of the slopes of the deflections as a function of impact parameters will then allow, via (4), to infer the two transverse sizes of the target beam to be tuned.

b. Form factor accounting for finite probe beam size

When the two beams are close, the average deflection measured in the BPM is reduced due to the finite size of the probe. This can be accounted for via the convolution of the probe density distribution with (2). The result of the calculation is summarized in two-dimensional form factors, by which the slopes in (4) are reduced, and given by

$$F_x(f, R_x, R_y) = F_y(1/f, R_y, R_x) =$$

$$\frac{1+f}{2} \int_0^\infty \frac{dt}{(1+t)[1+R_x^2+t]^{1/2}[f^2(1+R_y^2)+t]^{1/2}} \tag{5}$$

where R_x and R_y are the ratios of probe to target transverse sizes in both planes ($R_{x,y} = \sigma_{P_{x,y}}/\sigma_{T_{x,y}}$). As is consistent, the form factors become one for small $R_{x,y}$ and zero for large $R_{x,y}$. The functions are shown in fig. 6 and 7 for target aspect ratios $f = .1$ and $f = 1$.

In the special and initially unlikely case of round target and probe beams ($R_x = R_y = R, f = 1$), (5) reduces to

$$F_{Round}(R) = \frac{\mathrm{Log}\,(1+R^2)}{R^2} \tag{6}$$

The corresponding plot is shown in fig. 8.

III Application to SLC : Numbers and Ranges of Utilization

a. Limitations

Three types of limitations are anticipated. The main and most obvious one is the performance of the measuring BPMs. The better their resolution, the smaller the measurable offsets and the more effective the method. We hope for 20 μm or better on a single pulse. Particular attention has to be payed to their directivity, since beams will be measured from both directions. Harmful synchrotron radiation present in the environment will furthermore have to be masked.

The second limitation, the stability of the beams, is a fundamental limitation of SLC and is common to all colliding beam diagnostic and tuning procedures

A third difficuly arises from the non-gaussian, assymmetric distributions expected as a result of Linac wakefields and Arc non-linearities. Beam finding at large impact parameters is not affected, but the pattern of deflections shown in fig. 2 and 3 will be distorted to the extent that a lot of charge is carried by the tail. This and uncorrelated tilted $x - y$ distributions of the two beams, due to errors, will make the patterns hard to interpret. Fortunately, tuning for maximum slopes will always lead us in the right direction in the same way as beamstrahlung can be tuned for maximum emission power.

b. Scaling laws and relation to luminosity

The scaling laws are more favorable at low luminosities for this technique than for other beam-beam related signals.

The deflection at large impact parameters, which will be used for initial beam finding, scales as N_T/Δ, as can be seen from (3).

The maximum deflection produced as we scan the beams across each other to minimize spot sizes scales as N_T/σ_T, or as the root of luminosity.

c. Beam finding and centering

Initially, a first SLC beam will be threaded, at low repetition rate and intensity, through Arc and FFS, and to its dump. After best possible optimization of transmission and optical parameters, the above operation will be repeated with the other beam. BPMs on both sides will then be used to match the two orbit as well as possible. After this is done, the two beams will miss each other at the IP by offsets of a few hundred microns, which accounts for limited absolute BPM accuracy and alignment errors.

Bringing the two beams into collision, in preparation for spot size measurements,

will have to be done at full intensity since upstream wakefields, which affect the parameters to be tuned, are intensity dependant. Turning one of the two beams off momentarily will then produce an offset of

$$\Delta R^{BPM} \simeq \frac{-2N_T r_e}{\gamma} \frac{1}{\Delta} d_{IP \to \mathrm{BPM}} \tag{7}$$

in the BPM located 2.5 meters away. When this offset is large enough to be resolved, so that we know that the beams feel each other, they can be centered by mapping out two dimensional surfaces similar to those shown in fig. 3 to 5, in order to find the symmetry points.

Assuming $20\,\mu$m resolution, the range of utilization can be written

$$\frac{N_T[5 \cdot 10^{10}]}{\Delta[100\,\mu\mathrm{m}]} \gtrsim \quad 2.8 \tag{8}$$

This means that at $N_T = 5 \cdot 10^{10}$, signals will be measurable when the beams pass within $350\,\mu$m of each other.

c. Spot size minimization

The maximum offset produced in the BPMs, during the above described mapping can be approximated by

$$\left|\Delta R^{BPM}\right|_{\max} \simeq \frac{2N_T r_e}{\gamma \sigma_T} \cdot F_{Round}(1) \cdot d_{IP \to \mathrm{BPM}} \tag{9}$$

or

$$\left|\Delta R^{BPM}\right|_{\max}[\mu\mathrm{m}] \simeq 2000 \frac{N_T[5 \cdot 10^{10}]}{\sigma_T[2.5\,\mu\mathrm{m}]} \tag{10}$$

Also here assuming $20\,\mu$m resolution, the range covered is

$$\frac{N_T[5 \cdot 10^{10}]}{\sigma_T[2.5\,\mu\mathrm{m}]} \gtrsim \quad 10^{-2} \tag{11}$$

which corresponds to a luminosity of $4 \cdot 10^{25}\,\mathrm{cm}^{-2}s^{-1}$.

References

(1) P. Bambade, These de Doctorat 3eme Cycle, Centre d'Orsay (1984)

(2) For example : S. Kheifets , Petra-Note 119 (1976)

Acknowledgements

Many useful discussions with G. Bonvicini, G. Bowden, R. Erickson, H. DeStaebler and A. Minten are eagerly acknowledged. K. Bane suggested useful tricks for calculating some of the integrals.

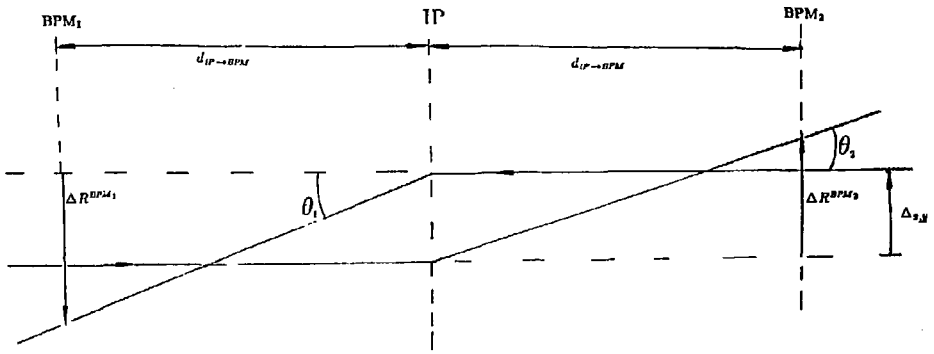
BPM1
IP
BPM2
$d_{IP\to BPM}$
$d_{IP\to BPM}$
θ_2
θ_1
ΔR^{BPM_1}
ΔR^{BPM_2}
$\Delta_{2,N}$

fig. 1

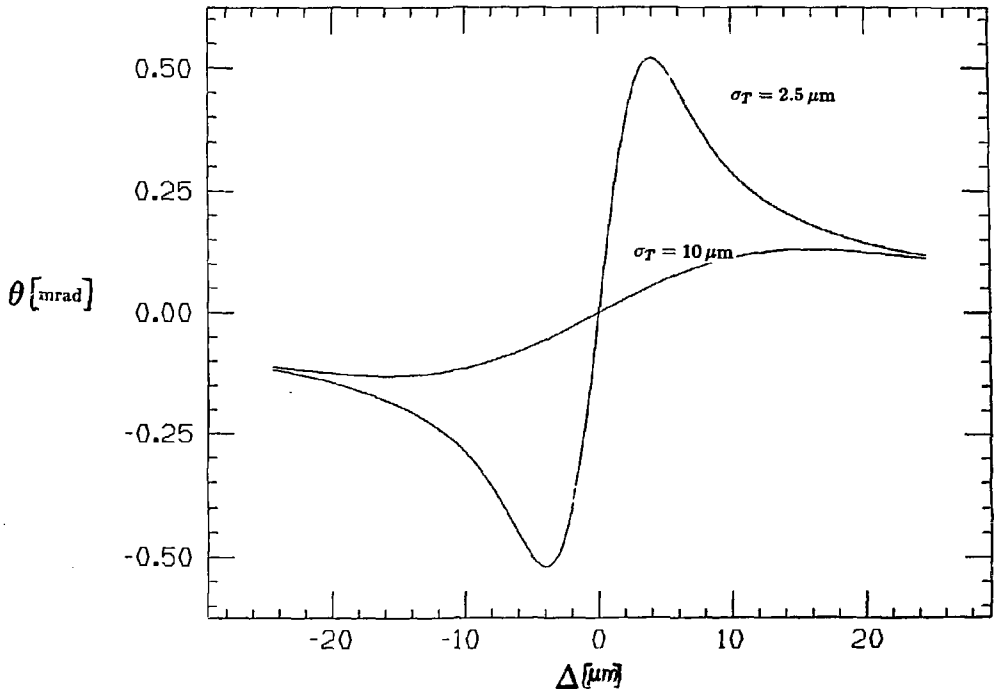

fig. 2: $f = 1$
$N_T = 5 \cdot 10^{10}$

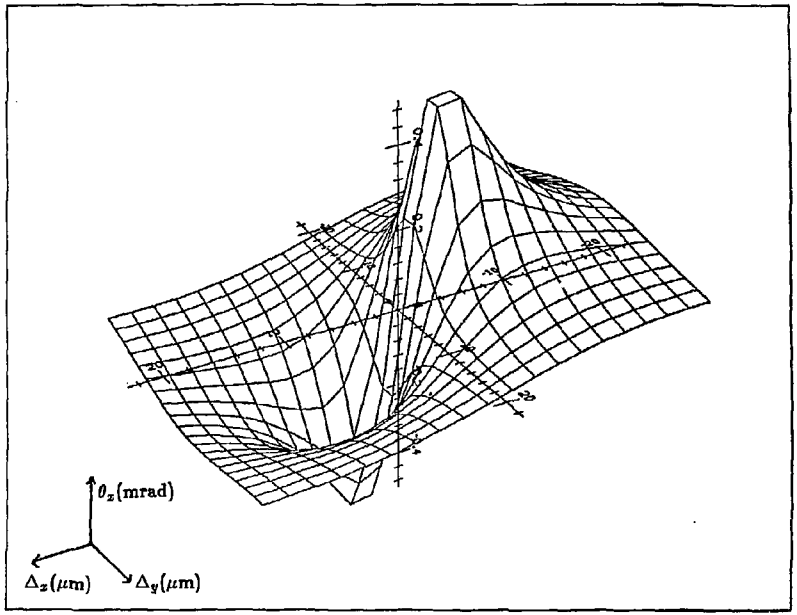

fig. 3.a:

$\sigma_{T_z} = 2.5\,\mu m$

$N_T = 5 \cdot 10^{10}$

$f = 1$

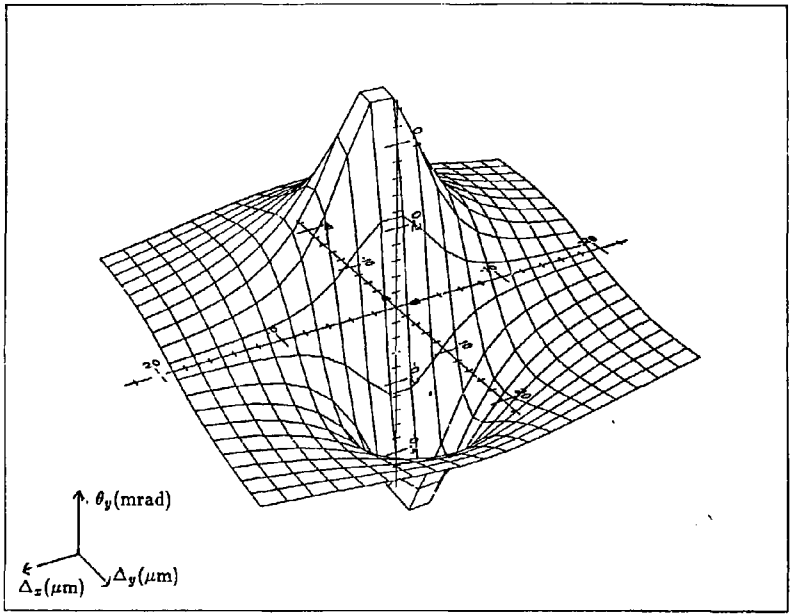

fig. 3.b.:

$\sigma_{T_x} = 2.5\,\mu$m
$N_T = 5 \cdot 10^{10}$
$f = 1$

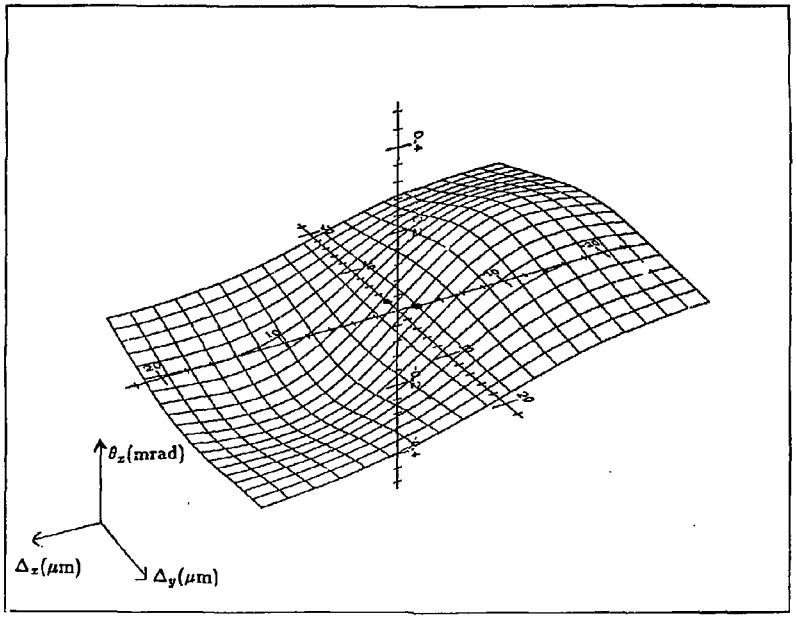

fig. 4.a: $\sigma_{T_x} = 7.5\,\mu m$

$N_T = 5 \cdot 10^{10}$

$f = 1$

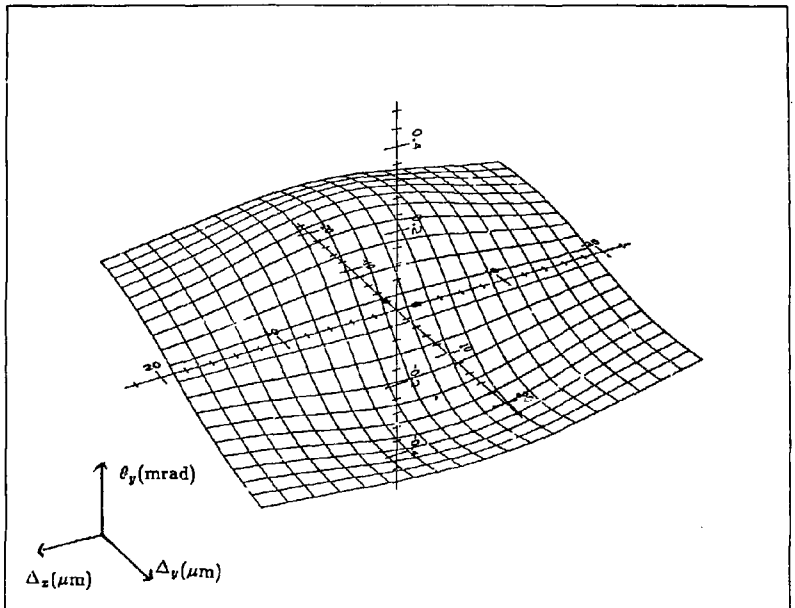

fig. 4.b: $\sigma_{T_z} = 7.5\,\mu m$

$N_T = 5 \cdot 10^{10}$

$f = 1$

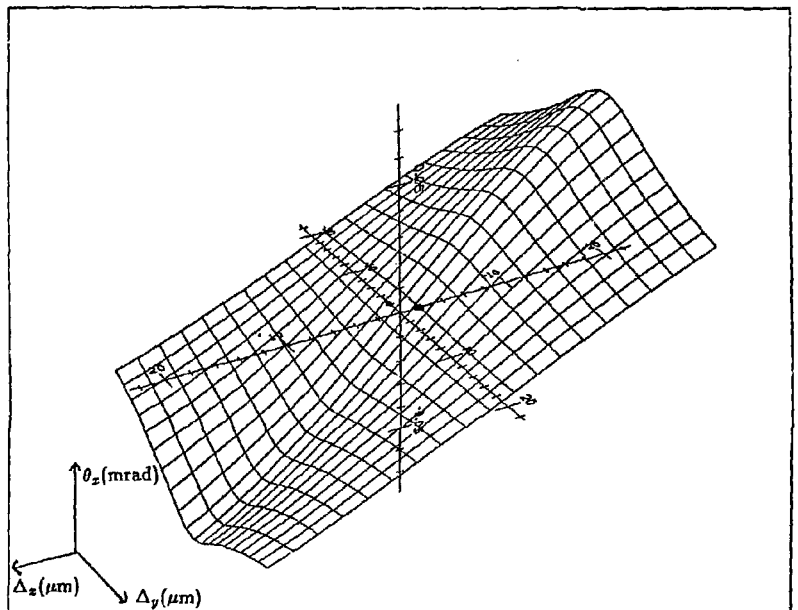

fig. 5.a:

$\sigma_{T_z} = 2.5\,\mu m$

$N_T = 5 \cdot 10^{10}$

$f = 1/10$

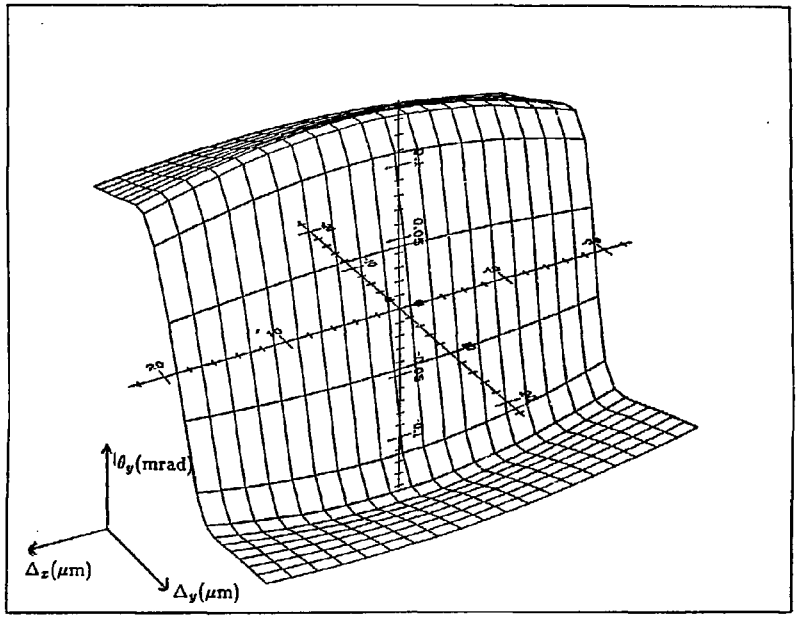

fig. 5.b:

$\sigma_{T_z} = 25\,\mu m$

$N_T = 5 \cdot 10^{10}$

$f = 1/10$

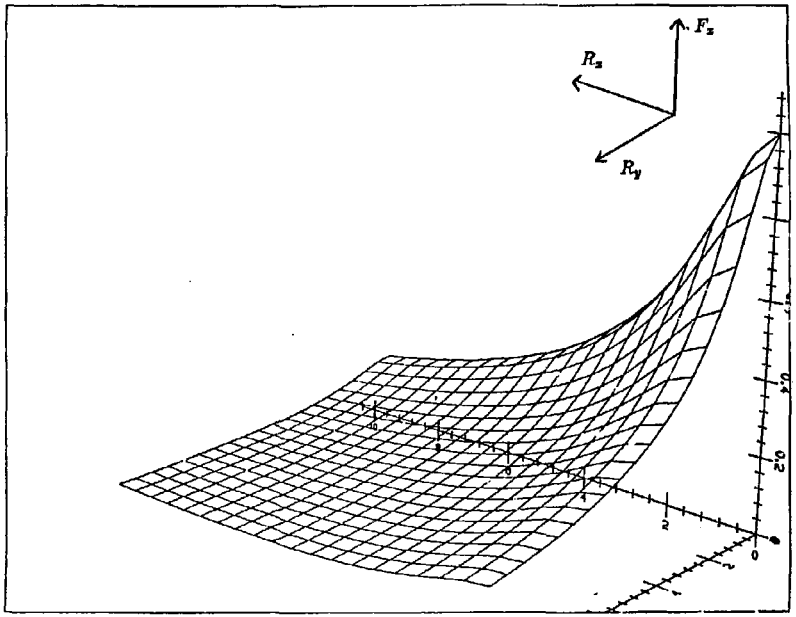

fig. 6: $f = 1$

$$R_{x,y} = \frac{\sigma_{P_{x,y}}}{\sigma_{T_{x,y}}}$$

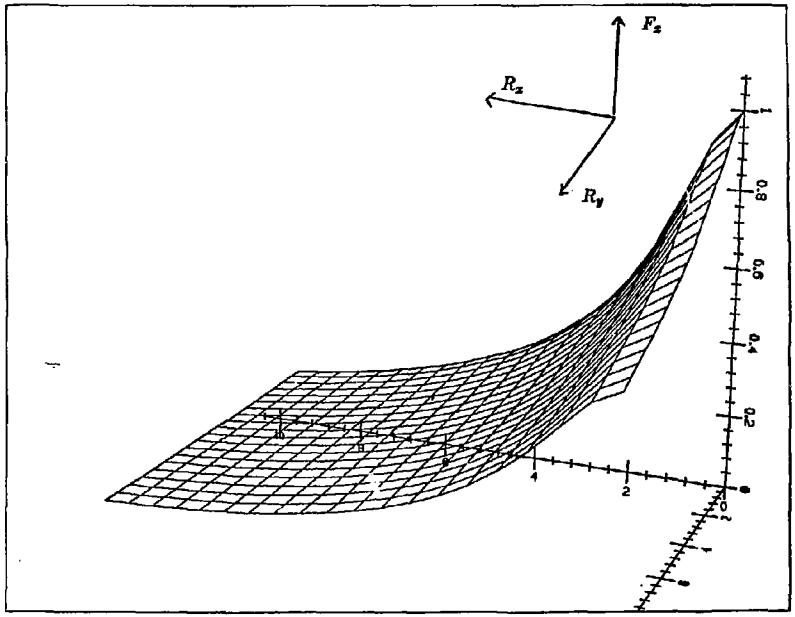

fig. 7: $f = 1/10$

$$R_{x,y} = \frac{\sigma_{P_{x,y}}}{\sigma_{T_{x,y}}}$$

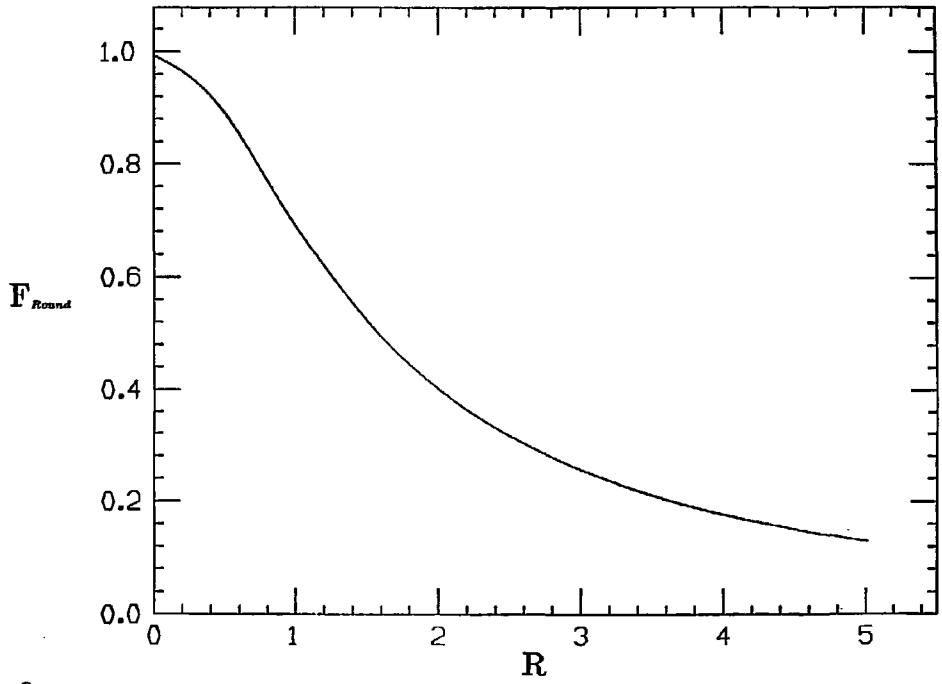

fig. 8: $f = 1$

$R_x = R_y = R$